

# FEASIBILITY STUDY OF ONCE-THROUGH COOLING FOR SOLAR THERMAL POWER PLANT ON THE LOWER ORANGE RIVER

Abiola G. Kehinde<sup>1</sup>, and Jaap Hoffmann<sup>2</sup>

<sup>1</sup> Solar Thermal Energy Research Group (STERG), Department of Mechanical and Mechatronic Engineering, Private Bag X1, MATIELAND 7602, South Africa; Phone: +27616551152; E-Mail: 20851634@sun.ac.za

<sup>2</sup> University of Stellenbosch, Mechanical and Industrial Engineering Building, Stellenbosch, South Africa; Phone: +27825789317; Fax: 0866155206; E-Mail: hoffmaj@sun.ac.za

## Abstract

Flood irrigation along the lower Orange River opens the opportunity to use water that was already extracted from the river system for condenser cooling. All the water is returned to the irrigation canal after passing through the condenser. Since the water is not returned to the river, temperature restrictions on water outlet temperature can be relaxed. No water treatment, other than screening was assumed, resulting in higher than normal fouling of condenser tubes. Annual average water use for irrigation is sufficient to serve a small number of medium to large solar thermal power stations. The lower condensing temperatures achievable through direct water cooling increased the thermal efficiency of the plant by almost 3 % compared to a solar thermal power plant fitted with a direct air cooled condenser. Furthermore, the seasonal range of water temperature varies between 20 and 25 °C which is small compared the changes in air temperature. Consequently, plant output remains fairly constant throughout the year. The plant considered was a hypothetical 50 MW<sub>e</sub> central receiver plant, with a live steam pressure and temperature of 130 MPa of inlet pressure and 540 °C

*Keywords: Once-through cooling; solar thermal power plant; irrigation; improved thermal efficiency; cooling water temperature; fouling.*

## 1. Introduction

Concentrated solar power (CSP) plants are built in arid regions with a good solar resource. In such regions, water is scarce, and CSP plants rely increasingly on dry cooling. In South Africa, all CSP plant use direct air cooling, except Bokpoort, that has a wet evaporative cooling system. The large terminal temperature difference, typically larger than 25 °C [1] at an air cooled condenser affects the thermal efficiency of these plants adversely, which may result in a significant loss of income. In evaporative (wet) cooling tower, the approach (difference between water outlet and dry-bulb temperature) is typically smaller than 10 °C [2]. Hence the thermal efficiency of

wet cooled power plant is about 3 % higher than that of a dry-cooled plant, but water consumption is almost 90 % higher [3].

Once-through cooling is in general not considered for solar thermal power plants, as these plants are usually situated in arid regions where water is scarce. High turbidity due to fog and humidity rule out coastal sites, especially for central receiver plant. Environmental legislation imposes severe restrictions on the maximum allowable temperature increase, should water be returned to a river system to protect aquatic organisms living in the water [4]. As a result, large amount of water has to pass through the condenser to keep the condenser outlet temperature down. Furthermore, no chemical treatment of the water is allowed if it is returned to the river.

In South Africa, 8 % of allocated water is used by industry and power generation, 18 % for municipal use and 62 % for agriculture and irrigation [5, 6]. Agriculture and irrigation are responsible for the bulk of water consumption in South Africa, and offers an opportunity if one can tap into it, without actually consuming the water. According to Kenny et al. [7], once-through cooling consumes 7 % of the water used (boiler blow-down, mirror cleaning, sanitation, etc.) in power plants compared to 70 % for evaporative cooling.

South Africa's largest river, the Orange River, runs through the Northern Cape, the region that has the highest solar irradiation in the country. Flood irrigation and hence large volumes of water in the lower Orange River irrigation scheme, stretching from Prieska in the east to Onseepkans in the west, a distance of almost 300km. Water is extracted from the river for irrigation at the Boegoeberg Dam, Upington and Kakamas. Water from the lower Orange River is almost fully allocated for agricultural municipal and industrial use by users from South Africa and Namibia [6].

This paper explores the feasibility of using water earmarked for irrigation to cool a CSP plant, before the full quota of the water is returned to the irrigation canal(s). Once-through cooling is proposed, as no water is consumed in the cooling process. There is a need to look at the synergy between the irrigation

scheme and a hypothetical CSP plant. Restrictions on water temperature for agricultural purposes need to be fully understood, as it will determine the number of power stations can be potentially served by the irrigation system

The central receiver or power tower technology was adopted for this study. It is capacity of reaching a higher temperature than parabolic trough and linear Fresnel systems, and hence yields potential higher thermal efficiencies.

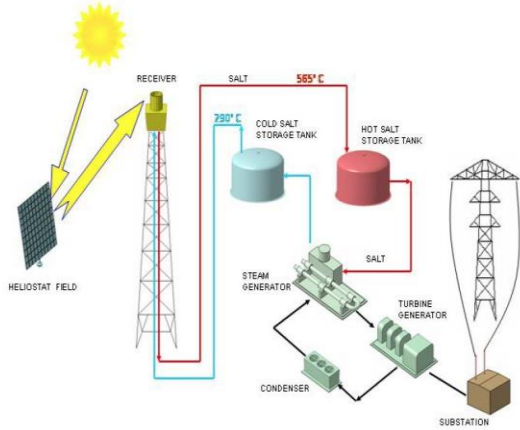


**Fig. 1: CSP central receiver plant [8]**

Figure 1 displays an example of a central receiver power plant. The central receiver power plant comprises of mirrors (heliostats) that track the sun about two axes, a central receiver to heat a heat transfer fluid (HTF) which in turn is used to heat the working fluid (steam) for a Rankine cycle.

## 2. Model description

### 2.1 Heliostat field

The site selected for this case study is Upington, a large town in the Northern Cape, on the Orange River. The coordinates and elevation for Upington is given in table 1.

Latitude	Longitude	Elevation
-28.395	21.2368	879

**Table 1: Site location**

Weather data for a typical meteorological year (TMY) for Upington was collected from the Solar Radiation Data [9]. Hourly averaged time step data was used to model CSP plant and it was assumed that the plant operate through successive steady states. Solar-PILOT software from National Renewable Energy laboratory (NREL) was used for design, characterization and optimization of concentrating solar power field geometry [10]. Weather data was provided in the format

required by Solar-PILOT. The heliostat field layout was set up at design-point (spring equinox), and DNI, solar azimuth and solar elevation angles were specified. Then the heliostat geometry, focus parameters, mirror performance parameters and optical error parameters were set to determine heliostat efficiency at the design point. To determine the annual efficiency of the heliostat field, time integration over a full year was performed. Parameters required for the integration were the hourly DNI over the year, and the position of sun (azimuth and altitude angle). The latter were calculated from Duffie and Beckman [11].

### 2.2 Central receiver

To determine the total energy received from the optical heliostat field, it is assumed that an external receiver is used with solar salt as heat transfer fluid. Crystallization of the salt mixture starts at 240 °C whilst the salt starts to decompose at temperature above 600 °C. The total heat received is calculated as:

$$\mathbb{Q}_{of} = (DNI)(\eta_{of})(A_{fa})(SM) \quad (1)$$

Where the field aperture area ( $A_{fa}$ ) is known as

$$A_{fa} = (H_t)(A_{he}) \quad (2)$$

There is no set up for the circumferential difference of the average heat flux on the receiver that will change throughout the day and the energy balance for the receivers that produces the heat transfers to the salt is determined.

$$(\alpha)\mathbb{Q}_{of} = \sigma\epsilon FA(\bar{T}_{mr}^4 - T_a^4) + UA_{ra}(T_{mrs} - T_a) + \mathbb{Q}_{salt} \quad (3)$$

It is assumed that the receiver heat flux  $q'_{max}$  is limited to 700 kW/m<sup>2</sup> as suggested by Sargent and Lundy LLC Consulting Group [12]. A receiver aspect ratio, ( $L/D$ ) of 1.6 was assumed, which allows one to calculate its height  $L$  and diameter  $D$  respectively. Overall heat transfer  $U$  is assumed to be approximately equal to the air side convective heat transfer coefficient. The receiver absorber area is conservatively taken as

$$A_{ra} = \pi LD \quad (4)$$

For radiation heat losses, it was assumed that the ground, air and surrounding structures are at ambient air temperature. Since the mean radiation temperature is much greater than the air temperature, the impact of this assumption will be insignificant. Also assumed that since the receiver is completely enclosed by its environment, the radiation shape factor will be 1 and the radiation loss is establish from the integration over the receiver surface presented by Hoffmann and Madaly [13].

$$\mathbb{Q}_{rad} = \sigma\epsilon \int_0^L [T^4(\xi) - T_a^4] \pi D d\xi$$

$$\begin{aligned}
&= \sigma \varepsilon \pi D \int_0^L T^4(\xi) d\xi - \sigma \varepsilon \pi D L T_a^4 \\
&= \sigma \varepsilon \pi D L (\bar{T}_{mr}^4 - T_a^4) \quad (5)
\end{aligned}$$

For a linear salt temperature distribution in the receiver, the mean radiation temperature at the receiver surface is calculated by

$$\begin{aligned}
\bar{T}_{mr}^4 &= \int_0^L T^4(\xi) d\xi \\
\bar{T}_{mr}^4 &= \frac{T_{max}^4 + T_{max}^3 T_{min} + T_{max}^2 T_{min}^2 + T_{max} T_{min}^3 + T_{min}^4}{5} \quad (6)
\end{aligned}$$

Where

$$\begin{aligned}
T_{max} &= T_{os} + \frac{2q'_{max} D_{or} \log(D_{or}/D_{ir})}{k_c} \\
T_{min} &= T_{is} + \frac{2q'_{max} D_{or} \log(D_{or}/D_{ir})}{k_c}
\end{aligned}$$

The receiver also experiences heat losses due to convection. To determine the convective loss which contains of natural and forced (wind focused) convection, a convective heat transfer coefficient is determined from

$$h = \sqrt{h_{nc}^2 + h_{fc}^2} \quad (7)$$

The convective heat transfer coefficient is reliant on the extent of the mixed velocity through the receiver which will recover both the limiting cases for forced convection when  $h_{nc}^2 = 0$  and natural convection for which  $h_{fc}^2 = 0$ . The Nusselt number presented in Çengel and Ghajar [14] for natural convection ( $Nu_{nc}$ ) is determined by Rayleigh number ( $Ra$ ) as

$$Nu_{nc} = \frac{h_{nc} D}{k_a} = 0.1 Ra^{1/3} \quad (8)$$

Where  $k_a$ , the thermal conductivity of air, and the air properties are calculated at the mean film temperature. The mean receiver surface temperature are also determined by

$$T_{mrs} \approx \frac{T_{os} + T_{is}}{2} + \frac{2q'_{max} D_{or} \log(D_{or}/D_{ir})}{k_{tm}} \quad (9)$$

The receiver is approximated as a cylinder. The forced convection heat transfer coefficient for flow across a circular cylinder presented by Zukauskas [14] is calculated as

$$Nu_{fc} = \frac{h_{fc} D}{k_a} = 0.027 Re^{0.805} Pr^{0.333} \quad (10)$$

The air properties are also calculated again at the mean film temperature due to the Reynolds  $Re$  and Prandtl numbers  $Pr$ . Where Reynolds number is defined as

$$Re = \frac{\rho V(y) D}{\mu} \quad (11)$$

The exact shape of the wind profile depends on the atmospheric stability, but for accessibility the wind speed at the receiver height is calculated from the 1/7<sup>th</sup> law for a neutral (adiabatic) atmosphere which is

$$V(y) = V_{10} \left(\frac{y}{10}\right)^{1/7} \quad (12)$$

Standard wind speed measurements are taken at 10 m above the ground level. Hence, convective loss is determined by

$$Q_{conv} = \pi D L h_{fc} (T_{mrs} - T_a) \quad (13)$$

### 2.3 Thermal energy storage

Figure 2 assumes that thermal energy storage loss is limited to the tank side wall, and only up to the salt level inside the tank. Since there is a direct connection between the salt inventories stored inside the tank and heat loss from the tank, assumed that the overall heat transfer coefficient is constant. That is  $U = 6 \text{ W/}^\circ\text{C}$  which bring about 1.5 % loss to the energy stored per day from a fully changed tank [15]. The thermal energy loss is given as

$$Q_{tel} = \pi D H_s U (\bar{T}_{ms} - T_a) \quad (14)$$

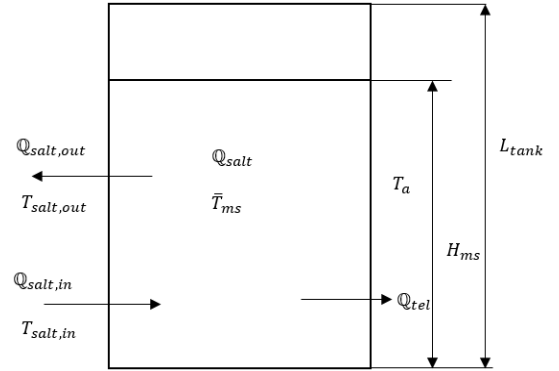


**Fig. 2: Schematic diagram of thermal energy storage**

Rodriguez et al [16] gives the comprehensive calculation of the heat losses in a storage tank. They assumed if the receiver heat flux is adequate for full load operation when the storage run out, the turbine will start again and this will partially offset the thermal lag of the solar thermal power plant. The amount of thermal energy stored per hour is determined by

$$Q_{tes} = Q_{salt,in} - Q_{tel} \quad (15)$$

### 2.4 Steam generation

From figure 3, it assumed that the preheater, evaporator, and super-heater in the steam generator are in series with a re-heater contained in parallel to the super-heater. Also, it is assumed that the exit salt temperature from the latter components is equal. The split in salt flow rate between the super-heater and re-heater is determined by the pinch to  $5 \text{ }^\circ\text{C}$  [17]. This value

was found from optimization of a heat recovery boiler [17] and may not directly apply to a molten salt steam generator. The hot salt temperature was limited to 565 °C and the cold salt temperature was not allowed to drop below 270 °C. The temperature of the cold salt differs in a narrow band around 273 °C. To calculate the salt flow rate, a heat balance was established from the inlet of the pre-heater to the super-heater and re-heater outlets on the steam generator.

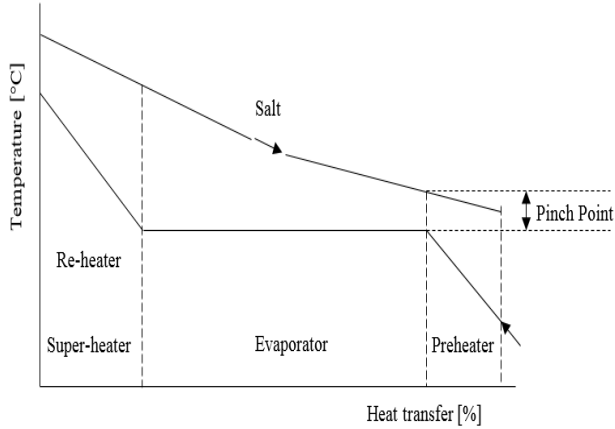


**Fig. 3: Schematic diagram of pinch point steam generator**

$$\dot{m}_s \bar{c}_{pmst} [T_{is} - (T_{sat} + \Delta T_p) - T_{os}] = \dot{m}_{hpt} (h_{sh} - h_{fw} + h_{ph}) + \dot{m}_{rh} \Delta h_{rh} \quad (16)$$

In equation (16),  $\Delta h_{rh}$  is the increase in enthalpy in the re-heater,  $h_{fw}$  is the saturated feed-water enthalpy entering the evaporator,  $\dot{m}_{rh}$  is the mass flow rate of the steam through the re-heater,  $h_{sh}$  is the steam enthalpy exit the super-heater,  $h_{ph}$  is the steam enthalpy entering the pre-heater,  $\dot{m}_{hpt}$ , the mass flow rate of the steam through the high pressure turbine,  $T_{sat}$ , the water/steam saturation temperature at the existence steam pressure,  $T_{is}$ , the inlet salt temperature,  $T_{os}$ , the outlet salt temperature,  $\bar{c}_{pmst}$ , the salt specific heat at the mean salt temperature, and  $\dot{m}_s$ , the mass flow rate of the salt.

## 2.5 Power block

The power block model assumes a single reheat Rankine cycle as shown in figure 4. The power block contains the following components: a steam generator, high, intermediate and low pressure steam turbines, electrical generator, condenser, feed-pump, and three feed-water heaters. The Microsoft Excel software with the add-in X steam [18] was used to calculate the thermodynamic properties of water and steam which includes temperature, pressure, entropy, enthalpy, and moisture content at all inlet and outlet of all components. The power block model is assumed to run through successive hourly steady states, with an instant step change between steady states, due to its small characteristic time relatively to the rate of change in DNI.

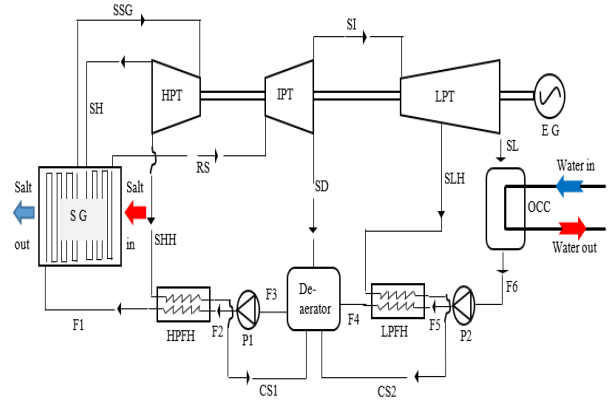


**Fig. 4: Schematic diagram of STPP power block**

The turbine used is based on the Siemens SST-800 series with a steam pressure of 130 bar and temperature of 540 °C [19]. The life steam states remains fixed at the maximum capacity rating of the turbine. The reheat pressure is assumed to be one quarter of the life steam pressure and the reheat temperature is the same as the inlet temperature of the high pressure turbines. The isentropic efficiency of the low, intermediate and high pressure turbines is assumed to be 90, 85 and 82 % respectively [19].

The plant is fitted with three feed-water heaters as shown in figure 4. It is assumed that the bled steam from the turbines condensed to saturated liquid in feed-water heaters, and is dumped directly into the de-aerator. It is assumed that the increase in temperature across all feed-water heaters are equal [20]. The isentropic efficiencies of both condensate extraction pump (P1) and feed-water pump (P2) is assumed 75 %.

A once-through surface condenser is assumed. It was modelled based on the parameters of a typical single shell, two pass condenser with Admiralty brass tubes given by Goodenough [21]. The condenser backpressure depends on the raw water temperature. It is also assumed that the properties of cooling water (river water) entering the condenser is the same as that of clean water. The total surface area of the tube and the material property are fixed, and it is assumed that there is no pressure drop across the condenser. Since the change in cooling water temperature is mainly seasonal and slow, the cooling water inlet temperature is kept constant during each time step. From the cooling water output temperature, the increase in temperature, the terminal temperature difference and initial temperature difference was determined. The fouling factor depends on water temperature, and was calculated from Goodenough's equation [21]. The power block was validated with SAM and showed a good correlation between both of them.

### 3. Model results

At design point, the heliostat field efficiency generated from the Solar-PILOT is at 46.90 %. The receiver loss is about 35 %. This is due to radiation and convection losses on the receiver. The effect of cooling water temperature on the power block performance is represented in figure 5. By varying the inlet cooling water temperature entering the condenser, the turbine output increased as the power block efficiency increased. At design point, the reference inlet cooling water temperature is 21.1 °C, the terminal temperature difference is 5 °C, the initial temperature difference is at 12 °C and the temperature difference between the inlet and outlet cooling water is calculated as 7 °C. From these conditions, table 2 is presented.

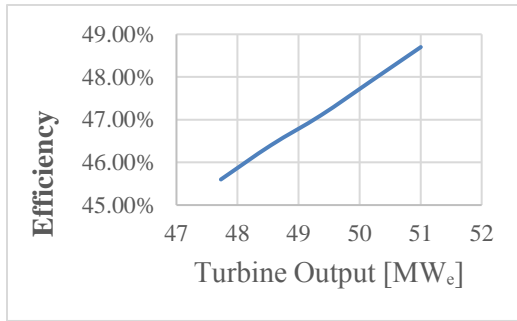


**Fig. 5: Effect of cooling water temperature on power block performance**

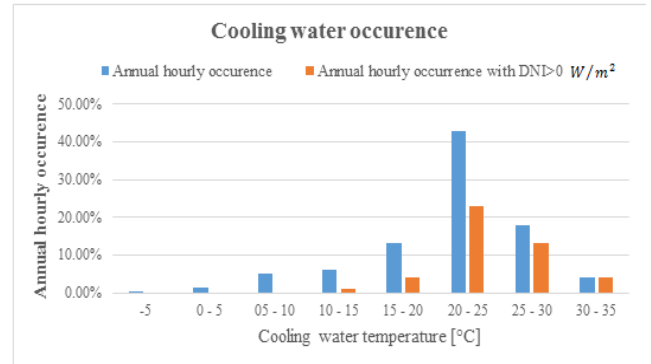
To prevent thermal pollution, the cooling water is not allowed to experience a temperature difference above 10 °C [22]. This make the condenser model become valid and appropriate for CSP plant.

	Units	Value
Energy supplied to steam generator	kJ/kg	104719.3
Efficiency	%	47.7
Outlet temperature	°C	28.1
Fouling factor	W/K	0.00131
Power output	MW <sub>e</sub>	50

**Table 2: STPP result at design point**

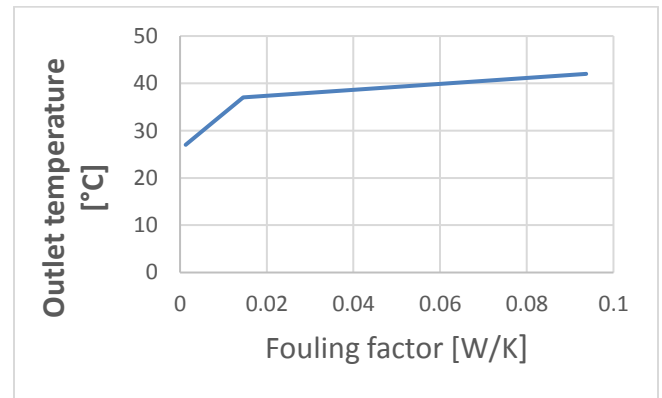
Based parameters in table 2, the outlet cooling water can return to irrigation system and be used for agricultural irrigation purposes. The analysis of hourly occurrence of the cooling water temperature experienced over the year from Orange River near Upington is represented in figure 6. It shows that the range of inlet cooling water temperature between 20 °C and 25 °C occurs frequently than other cooling water temperature collected from South African Weather Service (SAWS). In comparing this temperature with the range of hourly occurrence of the air ambient temperature (25-30 °C) experienced over the year, its shows that once through cooling has a greater advantage of improving the thermal performance of the CSP

plant than any other cooling systems. The same parameters was used to model CSP plant using air-cooled system and compared with once-through cooling system. It shows that there is an improvement in the thermal efficiency of once-through cooling CSP plant with a difference of 2.9 %.



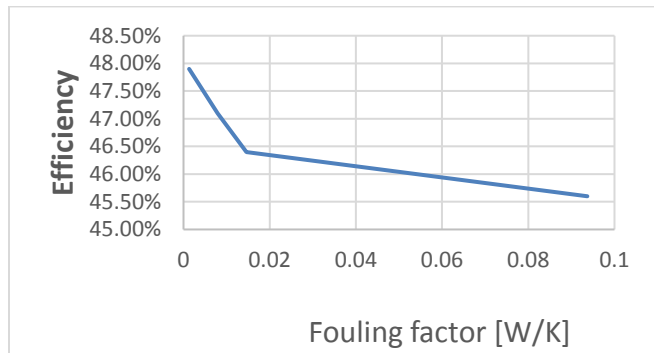
**Fig. 6: Annual hourly occurrence of inlet cooling water (Orange River) temperature**

Figure 7 shows the function of growth with temperature in the surface condenser. The growth occurs as a result of microbiological fouling and then kill-off as temperature increases.



**Fig. 7: Function of growth with temperature**

Figure 8 shows the performance of the power block against the condenser fouling at variable inlet cooling water temperature. As the temperature of the cooling water reduced, the resistance to condenser fouling reduced and there is an increase in the thermal efficiency of the CSP plant. The condenser fouling can be treated by softening or filtration.



**Fig. 8: The performance of the drop in thermal efficiency against condenser fouling factor**

The lower Orange River scheme uses 751 million cubic meters of water per year (a flow of about  $24 \text{ m}^3/\text{s}$ ) [4]. Based on the cooling water flow rate at design point which is  $2.24 \text{ m}^3/\text{s}$ , the design CSP plant will use about 70 million cubic meters of water per year. This means that the irrigated water can serve about 5 CSP plant using OTC system. This principle of using once through cooling for power plant can now solve the problem of power plant performance and at the same time still use the discharge water for agricultural irrigation purposes. Since the outlet cooling water is not returning to the eco-system (i.e. return back to the river), there wouldn't be any impact on the environment (eco-system). Then, the cooling water can be return to the irrigated canal or stored and used when needed or run it directly to the farm.

Over decades, environmental constraint has made once through cooling ineffective in power plant due to the government policy which does not allow new power plants to be constructed using water for cooling because the discharge cooling water can be harmful contaminants to the eco-system. Also, inability to prevent the aquatic animal living inside the water limit once-through cooling. But since there is an existing agricultural-irrigation system working perfectly in SA, this constraint can be totally avoided.

Based on agricultural constraint, there is no policy or law that constraint the use of irrigated water for CSP plant. No law that restrict not to discharge cooling water to the irrigation system. Then, it is assumed that the process is legal since law or policies were not broken. However, the withdraw water from the river for irrigation is not allow to be treated other than filtering or screening. This makes it possible to use the water for cooling in CSP plant.

#### 4. Conclusion

Once through cooling has potential to increase the performance of the CSP plant, since the temperature of the cooling water determine how efficient the CSP plant will be. Design

calculations, using once through cooling on a hypothetical CSP plant was done. This design will increase the production of electricity in South Africa and other parts of the world, provided that a suitable water source is available. Details are provided for each component of CSP plant that was used. Once through cooling was compared with air-cooling, and for this particular plant, and increase of almost 3 % in thermal efficiency was predicted.

As a result of restriction on the treatment of cooling water, condenser fouling is a potential problem and possible solution to reduce it was discussed. Trade-off between improved thermal efficiency against condenser fouling was done. The results show that condenser fouling has an effect on overall performance of the CSP plant. It shows a great advantage of using the cooling water coming out from the condenser for irrigation and agricultural purposes. An environmental and agricultural constraint was identified. Based on this study, a recommendation to use OTCS for CSP plant was made which will be a great benefit for the government and the entire people of SA.

#### 5. Acknowledgement

This research was supported by grants from National Research Foundation (NRF), the Solar Thermal Energy Research Group (STERG) and the Centre for Renewable and Sustainable Energy Studies (CRSES).

#### References

- [1] Pretorius, J.P. and Du Preez A.F., ESKOM cooling technologies, 14<sup>th</sup> IAHR Conference, Stellenbosch, 2009.
- [2] Chowdhury, B.A., Islam, M.S., Begum, F. and Parvez, A.M., Design and Performance Analysis of a Cooling Tower in Sulfuric Acid Plant, Journal of Chemical Engineering, Vol. 23, 2010.
- [3] Liqreina, A. and Qoadier, L., Dry Cooling of Concentrating Solar Power (CSP) Plants; An Economic Competitive Option for the Desert Regions of the MENA Region, Solar Energy, Vol. 103, pp. 417 – 424, 2014.
- [4] EPRI, “research and development relating to the generation, delivery and use of electricity for the benefit of the public. An independent, nonprofit organization, EPRI brings together its scientists and engineers as well as experts from academia and industry”. Available at: [http://eprijournal.com/wp-content/uploads/2015/07/Summer2013\\_Journal-low-3002001742.pdf](http://eprijournal.com/wp-content/uploads/2015/07/Summer2013_Journal-low-3002001742.pdf), 2013.
- [5] Roux, S. et al., “a Comparison of the Cost Associated With Pollution Prevention Measures”, 2012.

- [6] Water Affairs, “Vision of the National Water Research Strategy 2 Sustainable, equitable and secure water for a better life and environment for all”, p. 201. Available at: <http://www.dwa.gov.za/documents/Other/StrategicPlan/NWRS2-Final-email-version.pdf>, 2013.
- [7] Kenny, J. F. et al., “Estimated Use of Water in the United States in 2005 Circular 1344, Water”. Available at: <http://hbg.psu.edu/etc/Newsletter/doc/October2009.pdf>, 2009.
- [8] Cabeza, L. F. *et al.*, “Review of solar thermal storage techniques and associated heat transfer technologies BT - SPECIAL ISSUE: The Intermittency Challenge: Massive Energy Storage in a Sustainable Future”, 100(2), pp. 525–538. doi: 10.1109/JPROC.2011.2157883, 2012.
- [9] SoDa, “SoDa: a Web service on solar radiation”, (February). Available at: <http://www.soda-pro.com/>, 2018
- [10] NREL “SolarPILOT”, Available at: <https://www.nrel.gov/csp/solarpilot-download.html>, 2018
- [11] Duffie JA and Beckman WA, “Solar engineering of thermal processes”, 3rd Edition, Wiley, 2006.
- [12] Sargent and Lundy LLC Consulting Group, “Assessment of Parabolic Trough and Power Tower Solar Technology Cost and Performance Forecasts Assessment of Parabolic Trough and Power Tower Solar Technology Cost and Performance Forecasts - Report No. NREL/SR-550-34440 - National Renewable Energy Labora”, (October). doi: NREL/SR-550-34440, 2012.
- [13] Madaly K and Hoffmann JE, “Identifying the optimum storage capacity of a 100 MW CSP plant in South Africa”, 2014
- [14] Çengel, Y. A. and Ghajar, A. J. (2015) “Heat and Mass Transfer-Fundamentals & Applications”, Fifth Edit, 2015
- [15] Sioshansi R and Denholm P, The value of concentrating solar power and thermal energy storage, Technical Report, NREL-TP-6A2-45833, 2010.
- [16] Rodríguez I, Pérez-Segarra C, Oliva A, Torras S, and Lehmkuhl O, “Detailed numerical model for the resolution of molten salt storage tanks for CSP plants”, *Proceedings of 2nd International Conference on Solar Heating, Cooling and Buildings*, Rejika, 2012.
- [17] Behbahani-nia A, Sayadi S and M Soleymani, M, “Thermoeconomic optimization of the pinch point and gas-side velocity in heat recovery steam generators”, *Journal of Power and Energy*, 2010, 224(6), 761 – 771, 2010
- [18] Anonymous, (s.a), <http://xsteam.sourceforge.net/>, 2014.
- [19] Siemens, “Steam turbines for CSP plants”, p. 16. Available at: <http://www.energy.siemens.com/hq/pool/hq/power-generation/steam-turbines/downloads/steam-turbine-for-csp-plants-siemens.pdf>, 2011
- [20] Nag, P. K, “ Power plant engineering”, 3rd editio. New Delhi. McGraw-Hill Education, 2007
- [21] Goodenough J, “Thermal performance evaluation of artificial protective coatings applied to steam surface condenser tubes by”, December, 2013
- [22] Girish, S. *et al.*, “Analysis of a condenser in a thermal power plant for possible augmentation in its heat transfer performance”, *International Journal of Civil Engineering and Technology*, 8(7), pp. 410–420. Available at: <http://www.iaeme.com/IJCIET/issues.asp?JType=IJCIET&VType=8&IType=7>, 2017